The cilium-like region of the *Drosophila* spermatocyte: an emerging flagellum?

Marco Gottardo, Giuliano Callaini* and Maria Giovanna Riparbelli

Department of Life Sciences, University of Siena, Via A. Moro 4, 53100 Siena, Italy

*Author for correspondence (callaini@unisi.it)

Accepted 23 September 2013
Journal of Cell Science 126, 5441–5452

doi: 10.1242/jcs.136523

Summary

Primary cilia and flagella are distinct structures with different functions in eukaryotic cells. Despite the fact that they share similar basic organization and architecture, a direct developmental continuity among them has not been reported until now. The primary cilium is a dynamic structure that typically assembles and disassembles during mitotic cell cycles, whereas the sperm axoneme is nucleated by the centriole inherited by the differentiating spermatid at the end of meiosis. Fruit flies display a remarkable exception to this general rule. *Drosophila* spermatocytes have an unusual axoneme-based structure reminiscent of primary cilia (the cilium-like region, or CLR). This structure persists through the meiotic divisions when it is internalized with the centriole to organize the centrosome and is finally inherited by young spermatids. Examination of elongating spermatids by transmission electron microscopy (EM) and cold regrowth experiments suggests that the motile axoneme derives directly from the elongation and remodelling of the immotile CLR. Both the CLR and elongating spermatid flagella have incomplete C-tubules that form longitudinal sheets associated with the B-tubule wall, unlike axonemes of other organisms in which C-tubules stop growing at the transition between the basal body and the axonemal doublets. Moreover, both the CLR and spermatid flagella lack a structured transition zone, a characteristic feature of ciliated cells. *Uncoordinated (unc)* mutants that lack C-remnants have short centrioles, suggesting that the C-sheets play a role in the elongation of the centriole after it docks to the cell membrane. The structural similarities between CLR and sperm axoneme suggest that the CLR can be considered as the basal region of the future axoneme and could represent the start point for its elongation.

Key words: Cilium-like region, Flagellum, Male gametogenesis, *Drosophila*, *Unc*, *Klp10A*

Introduction

Cilia and flagella are membrane-bound organelles that are involved in several key cellular processes (Silverman and Leroux, 2009). Cilia act as paracrine signal transducers and mediate fluid flow, whereas flagella are actively involved in cell movement (Ishikawa and Marshall, 2011). Therefore, mutations in genes required for cilia and flagella assembly and function lead to many human diseases and developmental disorders (Bisgrove and Yost, 2006; Nigg and Raff, 2009). Although their general structure was described many years ago, the mechanism of their assembly has been clarified only in the past decade. Both cilia and flagella have an axial skeleton, the axoneme, an evolutionarily conserved structure composed of nine microtubule doublets. Whereas dynein arms emerging from the peripheral A-tubules and a central pair of microtubules characterize motile cilia and flagella, immotile primary cilia display only nine naked doublets. Because the growth of the axoneme takes place by the delivery of precursors to the tip of the growing microtubules, it was unclear how the new components reached their final positions. Studies in the green alga *Chlamydomonas* provided an elegant explanation: the ciliary axoneme is a highly dynamic structure, growing and shrinking by a unique system of bidirectional transport or intraflagellar transport (IFT) (Kozminski et al., 1993; Pazour et al., 2000; Rosenbaum and Witman, 2002). Conserved components of IFT have been found in most animals, suggesting that the IFT-dependent mechanism of axoneme assembly represents a widely distributed process in eukaryotes (Pedersen and Rosenbaum, 2008; Pedersen et al., 2008). The fundamental roles played by ciliary structures are thought to have imposed a strong pressure towards the evolution of the mechanisms that dictate axoneme architecture. Much is known about the IFT-dependent axoneme biogenesis in flagella of the green alga *Chlamydomonas* and in primary cilia of vertebrate cells, but these models probably cannot be directly transferred to understand the process of axoneme assembly and elongation in other organisms. Therefore, to obtain a general understanding of primary cilium formation, it is also necessary to investigate how ciliary axoneme assembly occurs in other organisms.

Drosophila represents a notable exception to the canonical rule of axoneme assembly, because IFT particles are needed for mechanosensory cilia formation but are not required for the sperm axoneme development (Han et al., 2003; Sarpal et al., 2003). This is remarkable considering the large supply of material that the assembly of a large flagellum demands. How, therefore, does the axoneme in *Drosophila* spermatids elongate? The bulk of the *Drosophila* spermatid axoneme is found within the cell cytoplasm, surrounded by a system of flat fenestrated cisternae that enable the in–out transit from the axoneme or cytoplasm compartments. This might suggest that axoneme growth depends upon the free diffusion of cytoplasmic components through the openings of the membranous sheath (Witman, 2003). However, the apical tip of the spermatid axoneme, where axonemal microtubules are assembled, is

surrounded by a continuous double-membrane sheath about 4–5 μm long that forms a ciliary pocket-like structure or CPL. This double sheath would make the proper addition or positioning of axonemal components by a simple diffusion mechanism difficult.

Drosophila has another kind of axoneme-based structure that projects out of the cell in primary spermatocytes (Tates, 1971; Fritz-Niggli and Suda, 1972). Because it is similar to a primary cilium, but differs in some structural aspects and properties, we propose to call it a cilium-like region, or CLR. Like primary cilia, the assembly and elongation of the CLR should require an IFT-mediated process. However, mutations in *Klp64D/Kif3A*, an anterograde kinesin motor protein required for cilium assembly, do not affect the structure of the CLR (Riparbelli et al., 2012). Thus, the dynamic of these structures might be independent of IFT, suggesting alternative mechanisms of axoneme elongation. In addition, the CLRs found on *Drosophila* spermatocytes break from the general rules of primary cilium biology. The CLR in *Drosophila* assembles in G2 phase and it is internalized during the meiotic division. Thus the centriole might organize the centrosome that drives the assembly of the spindle poles (Tates, 1971; Fritz-Niggli and Suda, 1972; Riparbelli et al., 2012; Carvalho-Santos et al., 2012; Roque et al., 2012; Fabian and Brill, 2012). This is in contrast to the prevailing view of the transient nature of the primary cilia correlated to cell cycle progression in vertebrate cells (Kim and Tsiokas, 2011; Kobayashi and Dynlacht, 2011). Moreover, all four centrioles assemble ciliary projections in spermatocytes. This is remarkable because it is generally assumed that only the mother centriole is able to nucleate a ciliary axoneme and that the daughter matures to this capability only 1.5 cell cycles later. Fragmentary observations of *Drosophila melanogaster* (Fritz-Niggli and Suda, 1972) and *Drosophila hydei* (Hennig and Kremer, 1990) male gametogenesis also hint at continuity between the CLR of primary and secondary spermatocytes and the flagellum of differentiating spermatids. Tokuyasu (Tokuyasu, 1975) hypothesised that ‘in insect spermatids, the assembly of the axoneme is completed within the short cilium’. Moreover, the single tubule within the spermatocyte CLR has been hypothesized to be the precursor of the central microtubule pair of the sperm axoneme (Carvalho-Santos et al., 2012).

The above observations conflict with general lines of evidence indicating that in most cell types the cilia are inconsistent with dividing cells and that the sperm axoneme assembles from the basal body during spermatid differentiation. We thus decided to carefully reinvestigate the structure and dynamics of the CLR and the process of sperm axoneme assembly in *Drosophila* using molecular markers for basal bodies and cilia, coupled with unequivocal ultrastructural imaging.

Our study reveals some unexpected findings. We show that the CLRs found in *Drosophila* spermatocytes lack the structural features of a true transition zone. Moreover, the C-tubules that terminate at the transition from basal body to axoneme in most ciliated eukaryotic cells (Fisch and Depuis-Williams, 2011) continue to grow and form longitudinal sheets coupled to the B-tubules.

The unusual disposition of the C-tubules persists in the spermatid axoneme where the wall of the A-tubule might act as a template for the B-tubule that, in turn, supports the assembly of the C-sheets. The specific features of the *Drosophila* ciliary axoneme are inherited in elongating spermatids. This points to a structural homogeneity between ciliary and spermatid axonemes, suggesting that during spermatid differentiation the CLR elongates to become the sperm axoneme.

Results

The unusual structure of the ciliary projections in the *Drosophila* spermatocytes

During male gametogenesis in *Drosophila melanogaster*, each primary spermatocyte has two pairs of centrioles that represent the platforms for the assembly of unusual ciliary projections (Fig. 1A, panels 1 and 2). Because these projections are reminiscent of primary cilia, but differ in some structural aspects and properties from a real cilium, we propose to call them cilium-like regions (CLRs).

Centrioles and CLRs reached their full length at the end of the first prophase (Fig. 1A, panel 1). The nine triplet microtubules of the centriole are immersed in a dense material that projected outwards from each triplet (Fig. 1B, panel 1). At the distal end of the centriole, thin threads of electron-dense material extended from the C tubule to contact the plasma membrane (Fig. 1B, panel 2). The transition from triplet into doublet microtubules took place at the distal end of the centriole (Fig. 1B, panel 3). The A and B tubules grew out, forming an axoneme that projected into the extracellular environment surrounded by the plasma membrane, whereas the C-tubules lost some of their protofilaments, growing into longitudinal sheets that persisted along the length of the cilium (Fig. 1A,C). Short lateral radial projections emerged from the B-tubule at a right angle to the C-remnants (Fig. 1B, panels 3 and 4). These projections did not reach the plasma membrane, but were seen to contact clusters of dense material that protruded from the inner wall of the ciliary membrane (Fig. 1, panels 3 and 4). The axoneme also displayed distinct links connecting the A and B tubules of adjacent doublets (Fig. 1, panel 4), reminiscent of the nexin links found in motile cilia. During the progression through the first prophase, both the axoneme and the centriole simultaneously elongated. The CLR internalized during the meiotic division (Fig. 1D) and the centriole might thus organize the centrosome that drives the assembly of the spindle poles. The membrane of the CLR was unsheathed by the cell membrane to form a distinct CPL.

A unique feature of centriole–CLR complexes was the usual presence of a long and wavy tubule that ran along the lumen of the centriole and inside the axoneme of the CLR (Fig. 1A, panel 1). The *Drosophila* spermatocyte CLR, unlike the usual 9+0 architecture of most animal primary cilia, therefore has an unconventional 9+1 structure.

Post-meiotic dynamics of the CLR

To track the dynamic of the centriole–CLR complex during male gametogenesis, we examined testes of flies expressing Unc-GFP fusion protein counterstained with an antibody against acetylated tubulin. At the end of prophase and during subsequent divisions three different domains of Unc-GFP localization were seen (Fig. 2A): a basal staining, corresponding to the mid-apical portion of the centriole, a intermediate bright dot-like signal and a distal labelling that colocalized with the acetylated tubulin signal.

Unlike most animal cells, in insect testis the second meiotic division occurs without centriole duplication, and thus consistently with a lack of DNA replication. Daughter secondary spermatocytes therefore have one centriole at each spindle pole and each young spermatid inherits only one centriole

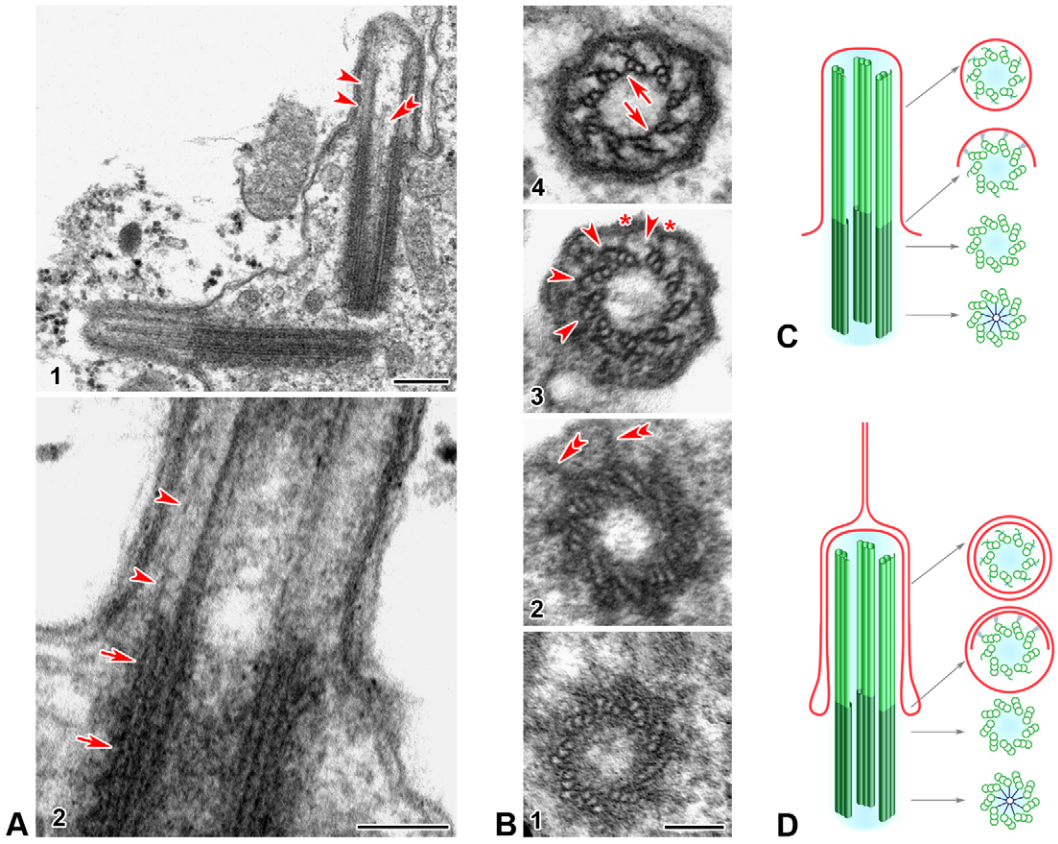

Fig. 1. Structure of the CLR in late primary spermatocytes. (A) Longitudinal sections of centriole–CLR complexes. (1) Orthogonal centriole/CLR complexes: note the single tubule crossing the centriole/ciliary lumen (double arrow) and the remnant of the C-tubule (arrowheads); (2) detail of the transition region between the centriole and the CLR: C-tubule (arrows), remnant of the C-tubule (arrowheads). (B) Cross sections through the centriole–CLR complex: (1) centriole; (2) apical region of the centriole showing dense fibers (double arrows) connecting the C-tubule to the plasma membrane; (3) basal region of the axoneme: note the gradual reduction of the C-tubule (arrowheads) and the short lateral projections (asterisks) close to the C-remnant; (4) distal region of the ciliary axoneme: note the distinct links (arrows) between the A- and B-tubules of adjacent doublets. Cartoons depicting centriole and CLR organization in primary prophase spermatocytes (C) and during meiotic divisions (D); centrioles are highlighted in darker green. Scale bars: 250 nm (A1); 100 nm (A2,B1–B4).

(Fuller, 1993), which maintained the three-domain pattern of Unc-GFP localization seen in mature spermatocytes (Fig. 2B, panel 1). As spermatids underwent elongation, the Unc-GFP distribution at the centriole changed, and appeared as three to four dots (Fig. 2B, panel 2). Very soon, the Unc-GFP dot and the associated distal staining separated from the centriole, leaving a narrow gap (Fig. 2B, panel 3) that increased further during spermatid elongation (Fig. 2B, panel 4). Double labelling with Unc-GFP and acetylated tubulin revealed that the Unc-GFP dot was positioned distally along the axoneme (Fig. 2B, panel 5). However, the Unc-GFP signal was never found at the tip of the axoneme even in fully elongated spermatids (Fig. 2B, panel 6), and appeared in cross optical sections as a ring-like structure surrounding the axoneme (Fig. 2B, panel 6, inset).

Axoneme continuity between CLR and spermatid flagellum

The internalized centriole–CLR complex was inherited at the end of meiosis by early spermatids (Fig. 3A, panels 1 and 2). The structure of the centriole was unchanged (Fig. 3A, panel 3) and the transition from triplet to doublet microtubules was marked by the reduction of C-tubules (Fig. 3A, panel 4), which formed thin longitudinal blades. Short lateral projections were still found. Both these structures were also present distally in the axoneme (Fig. 3A, panels 5 and 6). At the beginning of spermatid differentiation, the CLR lost the orderly array characteristic of the axonemal microtubules (Fig. 3A, panels 7 and 8). Thus, the ninefold symmetry was not maintained at the distal region of the axoneme as it starts to grow in early spermatids (Fig. 3A, panel 2).

Control spermatids, similar to those in panel 4 of Fig. 2B, showed a slightly elongated axoneme ending in a distinct CPL where the ninefold symmetry of the axoneme was disorganized (Fig. 3B, panel 1). The centriole had nine triplet microtubules with a distinct central tubule (Fig. 3B, panel 2) and the transition from centriolar triplets to axonemal doublets was marked by the gradual reduction of the C-tubule (Fig. 3B, panels 3 and 4). The C-tubule remnant was seen throughout the whole axoneme length in association with the B-tubule (Fig. 3B, panels 4–6) forming a lateral sheet that appeared progressively less complete from the base to the apex of the CLR. Thin lateral fibers orthogonal to the C-remnant were also seen in cross-section (Fig. 3B, panel 5). The B-tubule reduced distally, and at the tip of the axoneme, only isolated A-tubules were seen (Fig. 3B, panel 7). The axoneme lacked central pairs at this stage.

The central pair of microtubules that characterize the conventional 9+2 pattern organized at short distance from the

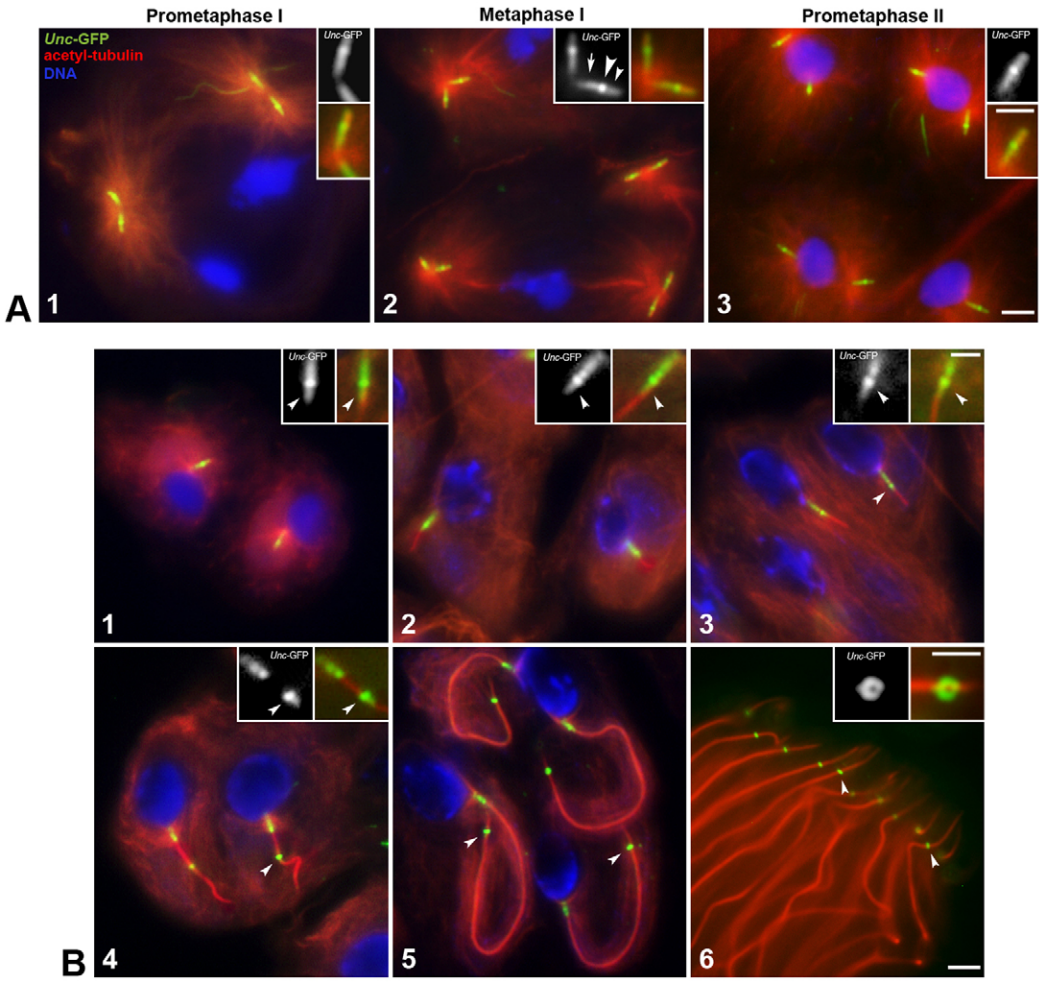

Fig. 2. CLRs persist into the spermatid stage, and then elongate. (A) Representative images showing centriole and CLR dynamics during progression through meiosis. (1) Prometaphase and (2) metaphase of the first meiosis; (3) prometaphase of the second meiosis; Unc-GFP is found at the mid-apical region of the centriole (arrow), within the CLR where acetylated-tubulin signal colocalizes (arrowhead) and at its basis (large arrowhead). (B) CLR dynamics during spermiogenesis. (1) In early spermatids, a small cluster of acetylated-tubulin colocalizes with the distal Unc-GFP labeling (arrowhead). As spermatids differentiate, the flagellum elongates (2) and extends well beyond the Unc-GFP at the distal centriole (arrowhead). As elongation of the flagellar axoneme proceeds (3,4), the subdistal and distal Unc-GFP labeling detaches from the centriole (arrowhead) and moves away along the axoneme. In elongating (5) and fully elongated (6) spermatids the dot-like Unc-GFP labeling reaches a subterminal localization along the axoneme (arrowheads). Unc-GFP localizes on a ring-shaped structure (inset 6). Unc-GFP is green, acetylated-tubulin is red, DNA is blue. Scale bars: 2.5 μm (A,B); 1.2 μm (inset B6).

centriole in elongating spermatids (Fig. 4A, panel 1). The centriole had a central tubule of variable length (Fig. 4A, panel 2) that extended within the basal region of the axoneme. This tubule might be shorter (n=11) or could reach the central doublets of the axoneme (n=15). Serial cross-sections from the distal end of the centriole displayed the partial loss of the C-tubules that form the laminar sheets visible as lateral projections emerging from the B-tubules (Fig. 4A, panels 3–6). Short lateral projections oriented towards the ciliary membrane appeared orthogonally to the C-tubule remnants (Fig. 4A, panel 6).

The distal portion of the growing axoneme was contained in a CPL of 4–5 μm in length (Fig. 4B, panel 1). The axoneme lost its 9+2 pattern in the proximal region of the CPL and extended in the distal region with single wavy and tangled tubules (Fig. 4B, panels 1 and 2). These tubules were often seen in contact with the electron-dense material at the tip of the CPL (Fig. 4B, panel 2). The radial projections and the sheets formed by the C-remnant persisted within the CPL in association with intact doublets (Fig. 4C, panels 1–5). The transition from doublets to single A-tubules (Fig. 4C, panels 6–8) was preceded by the disappearance of the C-remnant (Fig. 4C, panel 4) and then, in turn, by the progressive reduction of the B-tubule to an incomplete laminar sheet (Fig. 4C, panels 5 and 6, 4D). In longitudinal sections the remnant of the B-tubule detached from the A-tubule and bent to contact electron-dense material beneath the plasma membrane (Fig. 4B, panel 2, 4E).

The CPL did not change significantly its length during spermatid elongation, although the extension of the 9+2 axoneme within the CPL increased (Fig. 4F, panel 1). The disorganized region of the axoneme with isolated tubules was restricted to the distal tip of the CPL. The basis of the CPL and the tubular mitochondrial derivatives were separated by a cluster of electron-dense material that extended into the space between the axoneme and the plasma membrane (Fig. 4F, panel 1). Thick

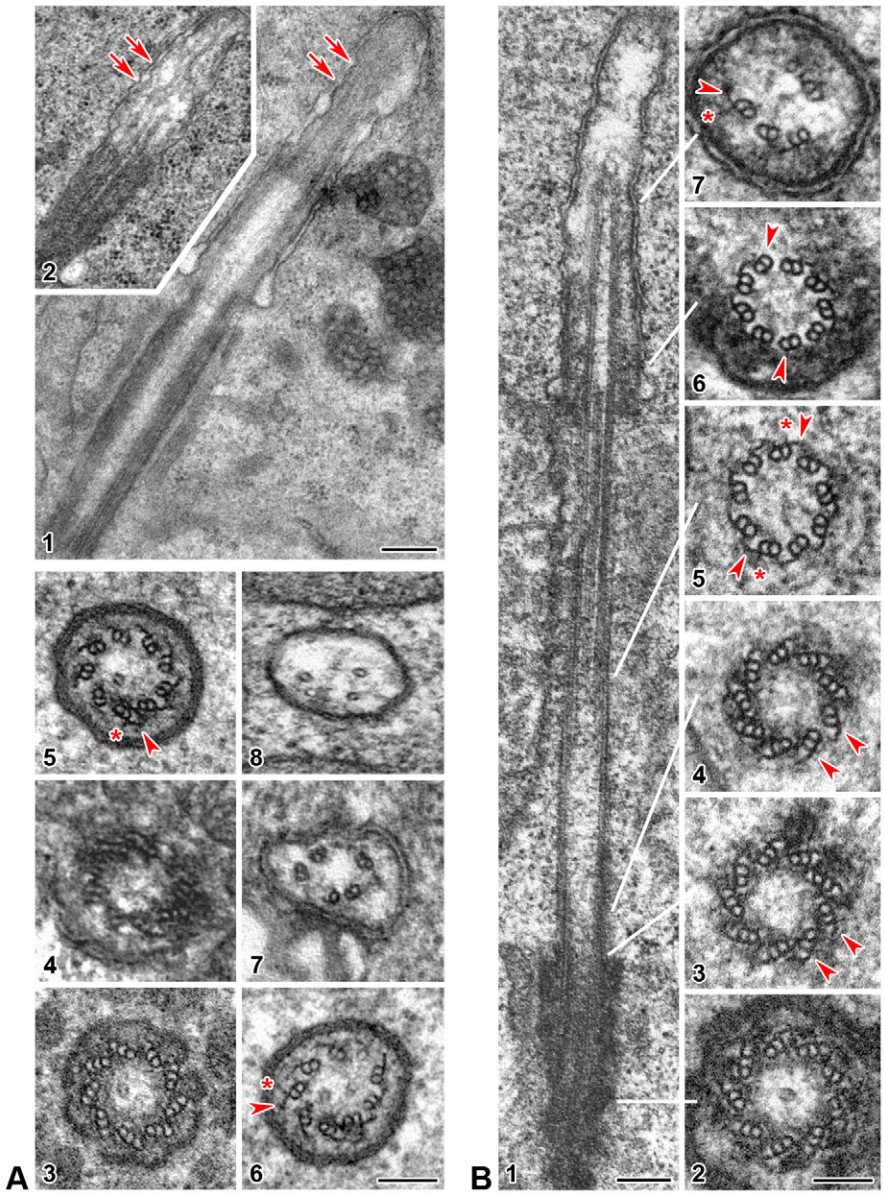

Fig. 3. CLRs reorganize in early spermatids. (A) Onion-stage spermatids (stage 13). (1,2) Longitudinal sections of the centriole and CLR show that the axonemal microtubules have lost their parallel arrangement and appear misoriented at the ciliary tip (arrows). (3–8) Cross sections of a centriole–CLR complex similar to that in panel 1 at the level of the basal region of the centriole (3), near the transition from centriole to CLR (4) and through the ciliary axoneme (5,6); note the thin lateral projections emerging from the microtubule doublets (asterisks) close to the C-remnants (arrowheads). The number of tubules decreases at the tip of the CLR (7,8). (B) Elongating control spermatid similar to those in Fig. 2B, panel 4. (1) The apical tip of the axoneme is enclosed in a distinct CPL formed by the ciliary membrane continuous with the plasma membrane; the axoneme is disorganized in the distal half of the CPL. (2–7) Representative cross sections from the centriole to the distal tip of the axoneme: (2) basal region of the centriole with a central tubule; (3,4) transition to the centriole triplets to axonemal doublets showing the progressive reduction of the C-tubule (arrowheads); (5) mid region of the axoneme with C-remnants (arrowheads) and lateral projections (asterisks); (6) base of the CPL: some doublets lack C-remnants (arrowheads); (7) distal region of the CPL: C-remnants (arrowhead) and lateral projections (asterisks) are still visible. Scale bars: 250 nm (A1–A2,B1); 100 nm (A3–A6,B2–B7).

connections of dense material were also seen between the ciliary membrane and the axonemal doublets or single tubules during earlier (Fig. 4F, panel 3) or later (Fig. 4F, panel 2) stages of spermatid elongation.

Microtubule regrowth at the distal end of the CPL

We next wondered whether the site of microtubule assembly was at the distal end of the axoneme. To address this question, we performed a microtubule re-growth assay in spermatids at various stages of elongation following cold-induced microtubule depolymerisation. After 45 minutes of cold treatment, most of the cytoplasmic microtubules depolymerised in elongating spermatids, with the exception of the axoneme microtubules. The pattern of acetylated tubulin was similar in untreated (Fig. 5A, panel 1), treated (Fig. 5A panel 2) and recovered (Fig. 5A, panel 3) young spermatids. The Unc-GFP dot moved along the axoneme of elongating spermatids but did not reach its distal end (Fig. 5A, panels 4 and 7). After cold treatment, the ring-shaped Unc-GFP signal (Fig. 5A, panel 5, inset) was localized at the extremity of the axoneme (Fig. 5A, panels 5 and 8). The presence of a distinct axoneme (Fig. 5A, panels 6 and 9) slightly shorter than in untreated spermatids was observed after recovery to room temperature for 5 minutes in cold-treated spermatids. The portion of the axoneme distal to the Unc-GFP dot was maintained in treated spermatids (Fig. 5A, panel 11), although slightly shorter than in recovered (Fig. 5A, panel 12) and untreated (Fig. 5A, panel 10) spermatids.

EM analysis of untreated spermatids like those in panel 4 of Fig. 5A showed that the 9+2 axoneme extended for a short tract in the CPL, whereas the remaining part was filled by wavy microtubules (Fig. 5B, panel 1). Axonemal microtubules of the most proximal region of the CPL were not affected by cold exposure, whereas the isolated distal ones were depolymerised (Fig. 5B, panel 2). The axoneme almost entirely crossed the ciliary CPL of spermatids at later stages of elongation, whereas isolated microtubules were only found at its distal tip.

CLR organization in mutants for genes involved in centriole assembly

Because the architecture of the CLR might reflect structural defects of the underlying centrioles, we examined male gametogenesis in mutants for genes involved in the regulation of centriole assembly. Thus, we can verify whether structural abnormalities are translated to the spermatid axoneme, confirming our hypothesis that CLR represents an intermediate stage in the assembly of the sperm axoneme. Moreover, this analysis could also supply new insights into the ultrastructure of the CLR and the role of the centriole in its assembly. To this aim, we decided to perform a detailed ultrastructural analysis of the CLR organization in primary spermatocytes and early spermatids in *Klp10A* and *uncoordinated* (*unc*) mutants that have opposite

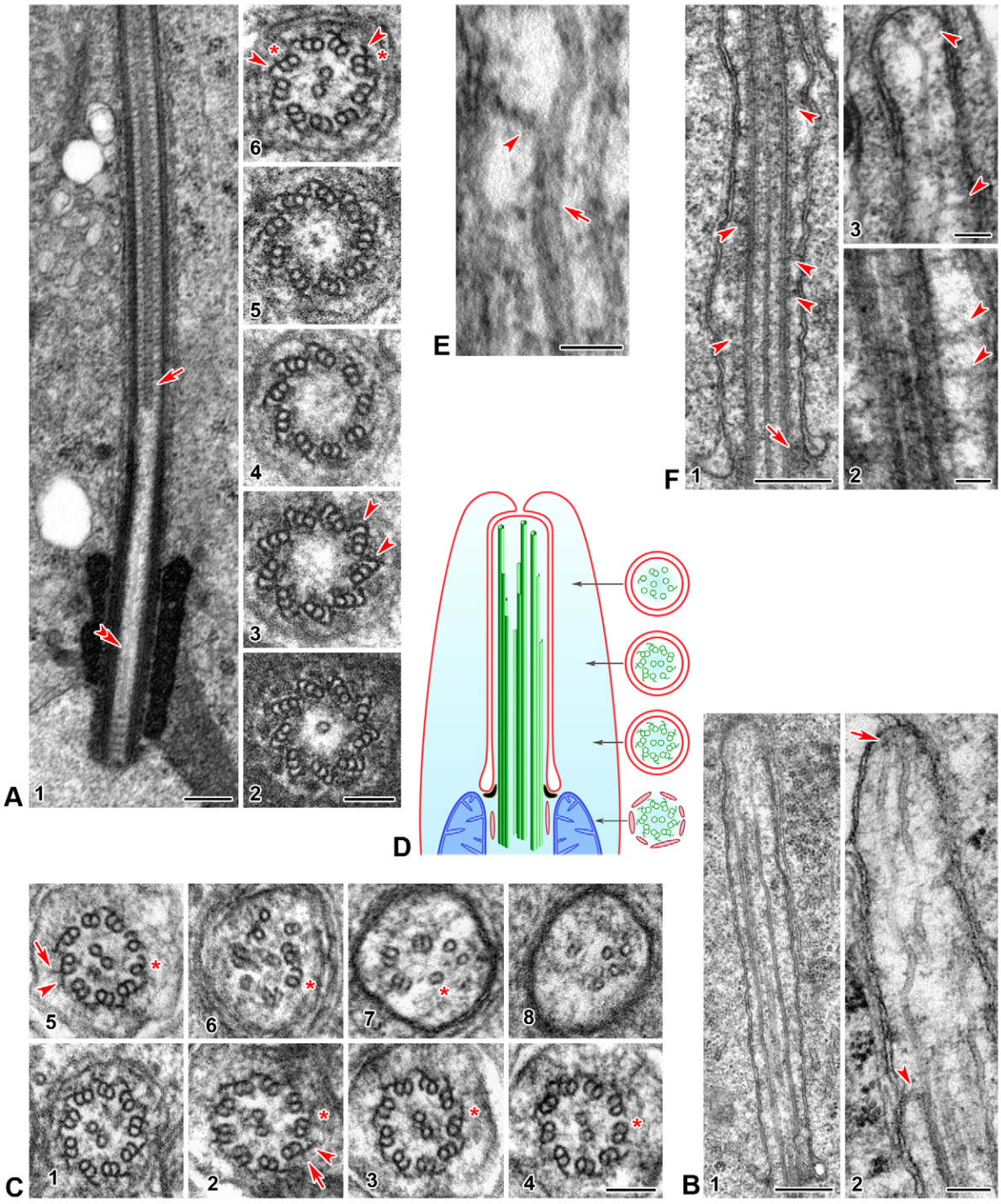

Fig. 4. See next page for legend.

phenotypes: extraordinarily long centrioles in *Klp10A* (Delgehyr et al., 2012) and unusually short centrioles in *unc* (Baker et al., 2004).

Although abnormal CLRs have been described in both *Klp10A* (Delgehyr et al., 2012) and *unc* (Baker et al., 2004) mutant testes, their ultrastructure has not been analyzed in detail. Mutants for the microtubule-depolymerising kinesin-13 *Klp10A*, which interacts with CP110 to control centriole length, had elongated and abnormally shaped centrioles that organized irregular CLRs of reduced dimension and abnormal shape (Fig. 6A, panels 1 and 3). The centriole had the usual structure of nine triplet microtubules (Fig. 6B, panel 1), although its distal region may contain incomplete triplets (Fig. 6B, panel 2). The ciliary axoneme held both doublets and triplets (Fig. 6B, panels 3–5). This agrees with longitudinal sections in which a portion of the centriole extended into the CLR (Fig. 6, panels 1–3). This highlights a poorly organized transition region between the centriole and the ciliary axoneme. Although the CLRs appeared abnormal in *Klp10A* mutant spermatocytes, C-remnants and lateral projections span the whole axoneme as in wild-type cells (Fig. 6C). Spermatids at the onion stage inherited a short CLR and a very elongated centriole (Fig. 6D).

Both centrioles and CLRs were reduced in size in *unc* mutants, a gene encoding a distal centriole protein required for ciliogenesis and involved in the process of centriole or basal body conversion (Baker et al., 2004) (Fig. 7A). Centrioles had the conventional nine triplet microtubules of equal length (Fig. 7B, panels 1 and 2), but unlike controls, the C-tubules completely terminated at the basis of the CLR (Fig. 7B, panel 3). Thus, *unc* CLRs appear rather unique in structure, given the shorter length and the lack of both longitudinal sheets associated with the B-tubule and lateral projections (Fig. 7C). Distinct bridges linking A- and B-tubules of adjacent doublets (Fig. 7B, panels 4 and 5) are found as in control cilia. Additionally, the axoneme had doublets of different extensions that were readily observable in cross sections of the CLR tip (Fig. 7B, panels 5 and 6). In onion-stage *unc* spermatids, the short centriole (Fig. 7D, panel 1) was associated with a long CLR in which the axoneme was disorganized (Fig. 7D, panel 2). Mutant *unc* intermediate spermatids (stage 16) had an unstructured axoneme enclosed in a disproportionately elongated CPL (Fig. 7E, panel 1). The centriole was shorter than that in controls, although it was built as a rule by nine triplet microtubules and a central tubule (Fig. 7E, panel 2). The C-tubules terminated completely at the distal end of the centriole (Fig. 7E, panel 3) and as a result the axoneme doublets lack the laminar projections associated with the B-tubules (Fig. 7E, panels 4 and 5). A single central tubule was seen up to the distal end of the CPL (Fig. 7E, panel 4) where the axoneme loses its ninefold symmetry (Fig. 7E, panel 6).

Fig. 4. CLRs persist in elongating spermatids. (A) Detail of the proximal region of an elongating axoneme in an intermediate spermatid (stage 16). (1) Longitudinal section showing the centriole, a single tubule (double arrowhead) extending in the basal region of the axoneme and the central doublets (arrow). (2–6) Cross sections from the centriole to the beginning of the central microtubule pairs: (2) centriole; (3) transition from triplets to doublets: arrowheads point to reducing C-tubules; (4–5) axoneme without central tubules; (6) axoneme with central tubules: arrowheads and asterisks indicate C-remnants and lateral projections, respectively. (B) Longitudinal sections of the apical end of an intermediate spermatid (stage 16): (1) the axoneme symmetry is lost very quickly within the CPL and (2) single microtubules end in clusters of dense material (arrow) at the tip of the CPL; the arrowhead indicates a B-tubules that detaches from the A-tubule wall. (C) Cross sections from the basal region to the apical tip of the CPL in intermediate spermatid (stage 16) (1–8): C-remnants (arrowheads) and thin lateral projections (arrows) continue within the CPL: note the gradual reduction of C-remnant and B-tubule in the selected doublet (asterisks). (D) Cartoon depicting the microtubule architecture of the CLR in an intermediate spermatid similar to that in C. (E) Detail of the distal region of the CPL showing the detachment of a B-tubule (arrowheads) from the wall of an A-tubule (arrows). (F) Longitudinal sections of the CPL in late (stage 18) (1,2) and intermediate (stage 16) (3) spermatids: (1) the structured axoneme almost fills the length of the CPL, clusters of dense material localizes at the marginal zone of the CPL (arrow) and dense projections (arrowheads) link the axoneme with the plasma membrane; dense projections also link axonemal doublets (2, arrowheads) or single tubules (3, arrowheads). Scale bars: 250 nm (B1,F1); 200 nm (A1); 100 nm (A2–A6,B2,C1–C8,E,F3); 50 nm (F2).

Discussion

The distal end of the *Drosophila* centriole carries thin projections that remember in their position the transition fibers found at the basis of the primary cilium of most animal cells. However, whereas the transition fibers usually emerge from the B-tubules, the projections associated with the *Drosophila* centriole originate from the C-tubules. Despite the apparent divergence between the two structural organizations, these projections might have a similar functional significance. They seem to tether the centriole to the cell surface, and might define the boundaries between the plasma and the ciliary membranes in a similar manner to the distal appendages of the primary cilium in vertebrate cells (Sorokin, 1968; Dawe et al., 2007). In vertebrate cells, the transition fibers of primary cilia play a crucial role as filter barrier to regulate the free diffusion of cytoplasmic components inside the ciliary compartment (Reiter et al., 2012; Czarnecki and Shah, 2012; Szymanska and Johnson, 2012). We cannot exclude a similar function for the projections associated to the distal end of the *Drosophila* centriole. Interestingly, in *Drosophila* spermatocytes the membrane that surrounds the basal region of the CLR is particularly rich in vesicles that could represent a large stock of cytoplasmic components needed to refurnish the dynamic ciliary complex (Riparbelli et al., 2012). Therefore, this membrane domain might be an important site for vesicular trafficking from and to the plasma membrane, as occurs in the ciliary pocket of some vertebrate cells (Molla-Herman et al., 2010; Rohatgi and Snell, 2010; Benmerah, 2013).

Two closely interconnected features usually identify the transition from the basal body to the axoneme: the end of the C-tubule, along with the extension of A- and B-tubules. Surprisingly, the outer C-tubule does not stop growing at the beginning of the axoneme in *Drosophila* CLRs. It loses some protofilaments, reducing its size to form a continuous longitudinal sheet that runs along the whole axoneme in association with the B-tubule. The function of the C-remnant in the organization of the CLR is unclear, because this structure can assemble in *unc* mutants despite the C-tubule ends at the transition between the centriole and the ciliary axoneme. However, centrioles are shorter in *unc* mutants, suggesting that C-remnants play a role in the elongation of these organelles. Moreover, the lack of lateral projections points to the requirement of C-remnants. The *unc* phenotype might explain how centrioles and associated ciliary axonemes increase their length at the same time in *Drosophila* primary spermatocytes. This is a unique process, because in other animal cells whereas the primary cilium elongates, the basal body does not change

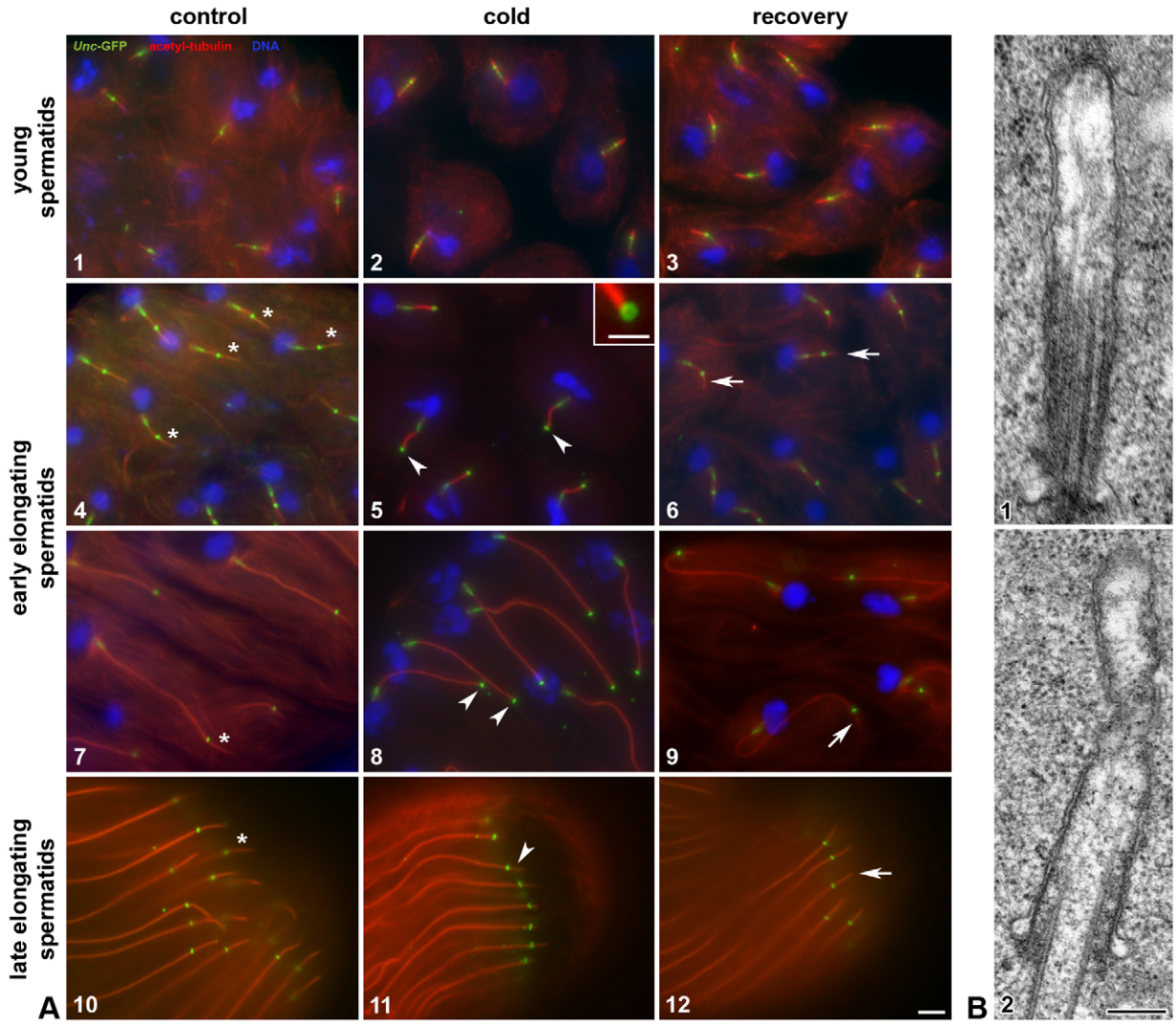

Fig. 5. Microtubules regrow at the apical tip of the axoneme after cold treatment. (A) Spermatids expressing Unc-GFP (green) were exposed to cold for 45 minutes and then recovered at 24°C for 5 minutes. Acetylated-tubulin is red and DNA is blue. Distinct microtubules are present distally to the Unc-GFP dot in untreated spermatids (asterisks) during the process of elongation. Cold exposure leads to the loss of such microtubules (arrowheads) that start to regrow after recovery (arrows). By contrast, cold treatment partially affects the distal microtubules during later stages of spermatid elongation: these microtubules are still visible (arrowheads), although shorter than that in untreated (asterisks) and recovered (arrows) spermatids. (B) Detail of the CPL in (1) cold-treated and (2) untreated spermatids. Scale bars: 2.5 µm (A); 1.2 µm (inset in A5); 250 nm (B).

dimensions after its docking at the plasma membrane. It can be hypothesized that during the elongation of the A- and B-tubules, cytoplasmic precursors of the missing protofilaments join to the C-sheet at the distal end of the centriole, thus completing the tubule and allowing centriole to elongate concurrently.

Thin radial projections emerge from the B-tubules at a right angle to the C-sheets. Projections associated to the axonemal doublets usually characterize the proximal region of the primary cilium of most organisms, the so-called ‘transition zone’. These projections are typically Y-shaped, emerge at the A- and B-tubule junction, and directly contact the ciliary plasma membrane (Gilula and Satir, 1972; Ringo, 1967). The projections found in the CLR of *Drosophila* spermatocytes emerge from the B-tubule, are L-shaped in cross section and do not contact the ciliary membrane. It is important to remark that these projections were found along the whole CLR in *Drosophila*. This condition contrasts with findings in other eukaryotic cells where Y-links are restricted to the ‘necklace’, a distinct region at the proximal base of the primary cilium (Reiter et al., 2012). The CLR of *Drosophila* spermatocytes somehow ‘remember’ the structure of the connecting cilium found in photoreceptors cells, where Y-shaped links extend along the cilium (Insinna and Besharse, 2008). Likewise, microtubule–membrane connections extending along much of the axoneme have been also described in *Leismania* amastigote flagella and in kidney primary cilia raising the possibility that both ciliary and flagellar axonemes represent extended transition zones (Gluenz et al., 2010).

It has been recently shown that in sensory neurons the coiled-coil protein Chibby (CBY) colocalizes at the distal end of the centriole with CG14870, the *Drosophila* ortholog of MKSR1, a component of the MKS module at the transition zone (Enjolras et al., 2012). Similar to typical transition zone components, CBY

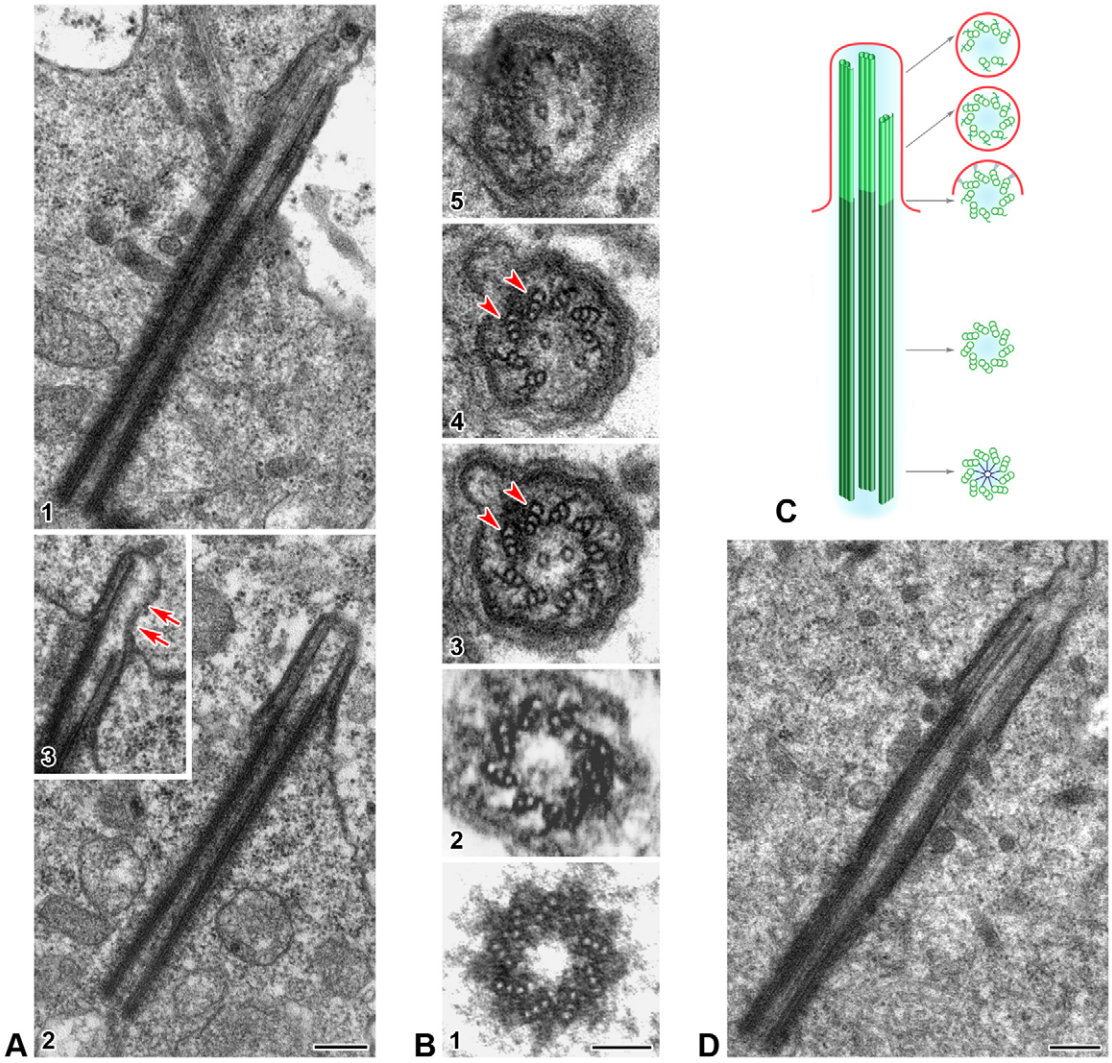

Fig. 6. The organization of the CLR in *Klp10A* mutant testes. (A) Longitudinal sections of centriole–CLR complexes in primary spermatocytes: (1,2) centrioles are unusually long and (3) the CLRs have an incomplete set of doublets (arrows). (B) Cross sections of the centriole–CLR complexes: (1) proximal and (2) distal region of the centriole: (3–5) basal to apical end of the CLR, note the persistence of some triplet microtubules (arrowheads) within the ciliary axoneme. (C) Schematic representation of a centriole–CLR complex in a primary prophase spermatocyte from *Klp10A* mutants. (D) *Klp10A* mutant spermatids at onion stage (stage 13) display very elongated centrioles and abnormal CLRs. Scale bars: 250 nm (A,D); 100 nm (B1–B5).

is required to regulate protein trafficking into and out sensory neuronal cilia. In *Drosophila* male germ cells, CBY was also found to colocalize with Unc at the distal end of the centriole, and in later stages, at the tip of the spermatid axoneme. It has been proposed that CBY is essential for proper centriole function and that, given its localization, both *Drosophila* CLR and sperm flagella might develop as elongated transition zones (Enjolras et al., 2012). Accordingly, there is evidence from different model systems that transition zone formation does not require intraflagellar transport (Reiter et al., 2012).

The unusual structural details found in the CLR of the *Drosophila* spermatocytes point to the lack of a conventional transition zone. This is consistent with the finding that the CG14870 gene product is associated with the distal end of the centriole in sensory neurons, but not in spermatocytes (Avidor-Reiss et al., 2004). However, we cannot exclude the possibility that a structure molecularly similar to a transition zone, but morphologically different, is assembled in *Drosophila* spermatocytes and maintained during spermatid elongation. Indeed, the appearance of the transition zone has been reported to vary between species and cell types, although the basic structural features appear to be conserved (Fisch and Depuis-Williams, 2011).

In *Drosophila* primary spermatocytes, the CLR elongates in the extracellular milieu and during the meiotic divisions internalizes into the cell by an invagination of the plasma membrane. A sheath with inner and outer membranes thus surrounds the ciliary axoneme inherited by young spermatids (Tates, 1971; Fritz-Niggli and Suda, 1972). This membrane invagination looks like the ciliary pocket that surrounds the proximal region of the primary cilium in several vertebrate cell types. However, despite the fact that these structures are morphologically related, they are not functionally equivalent. In fact, in *Drosophila* spermatids, the marginal zone of the CPL

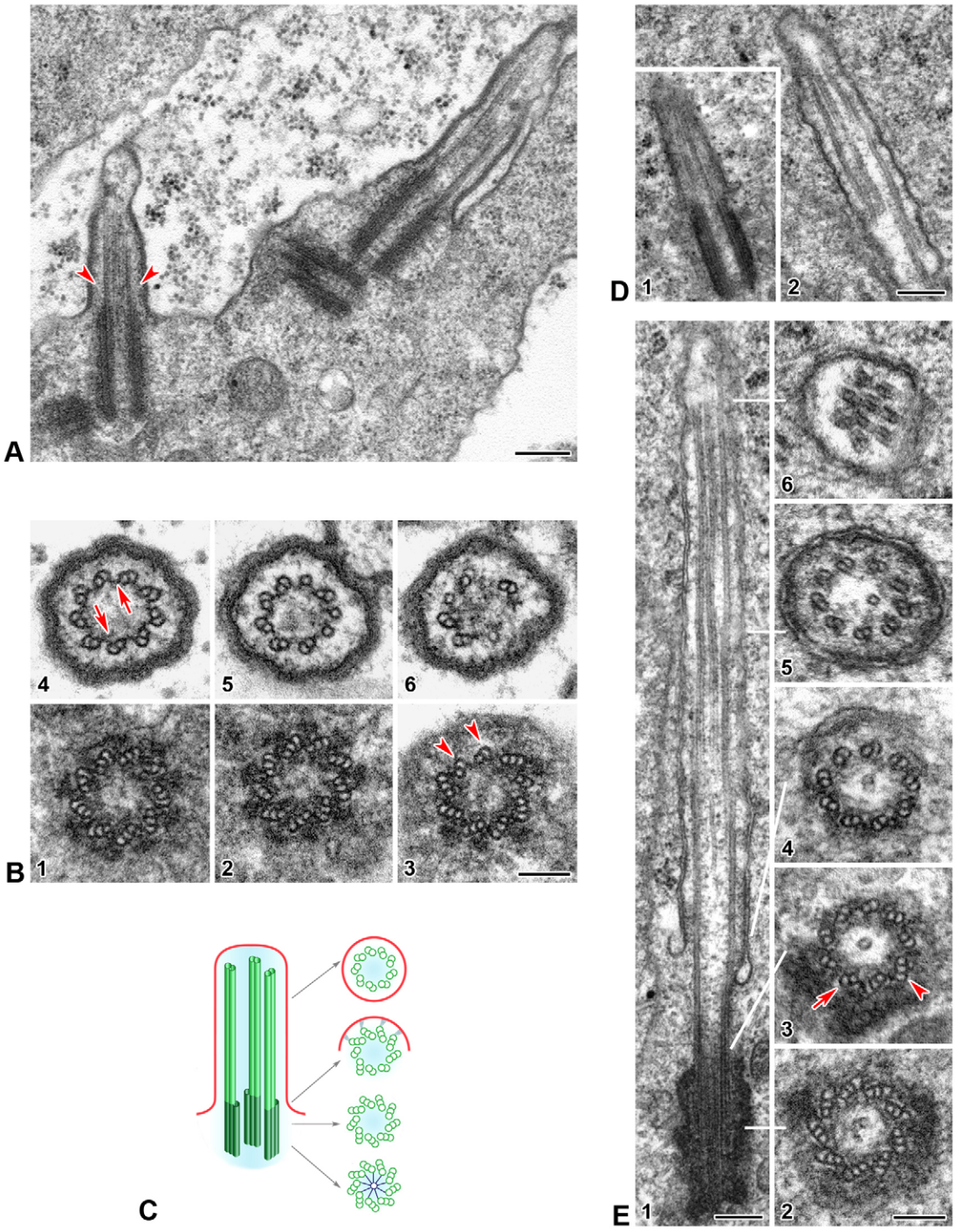

Fig. 7. Mutations in *unc* affect the structure of the CLR. (A) Longitudinal sections show the odd size of the centriole and the irregular shape of the CLR in primary spermatocytes: note the absence of the C-remnant (arrowheads). (B) Cross sections through the centriole–CLR complex: (1,2) centriole; (3) loss of the C-tubule (arrowheads) at the transition from the centriole to the ciliary axoneme; (4–6) organization of the ciliary axoneme at different levels: the adjacent microtubule doublets lack projections and are interconnected by distinct links (arrows). (C) Schematic representation of a centriole–CLR complex in a primary prophase spermatocyte from the *unc* mutant. (D) Longitudinal section of centriole–CLR complexes in early spermatids at onion stage: note the unusually short centrioles (1) and the disorganized ciliary axoneme (2). (E) Intermediate spermatids (stage 16). (1) Almost all the axoneme is enclosed in a strikingly extended CPL. (2–6) Representative cross sections from the centriole to the apical tip of the axoneme: (2) basal region of the centriole; (3) transition from the centriole to the axoneme: the C-tubule (arrowheads) quickly reduces (arrow) and axonemal doublets lack C-remnants; (4) basal, (5) middle, and (6) distal regions of the CPL; note the single tubule spanning from the centriole to the middle of the CPL. Scale bars: 250 nm (A,D,E1); 250 nm (B,E2–E6).

does not correspond to the membrane domain found at the basis of the primary cilia. An important point is that the CPL of *Drosophila* spermatids is not correlated to the ciliogenesis pathway, but instead it is a consequence of the inward invagination of the CLR during the meiotic progression. During early spermatid elongation, the Unc-GFP ring localized within the marginal zone of the CPL becomes free from the distal end of the centriole and was positioned toward the caudal end of the axoneme, tracking the leading edge of the CPL. Mutations in *unc* lead to the overgrowth of the CPL and the consequent reduction of the axoneme portion free in the cytoplasm. These data suggest that *unc* could be implicated in the complex dynamics of the CPL and in the maintenance of its shape.

Our observations revealed a few vesicles at the basis of the CPL, suggesting that vesicular trafficking does not play an important role in the process of axoneme elongation in *Drosophila* spermatids. By contrast, vesicle docking is usually required in vertebrate cells to ensure membrane expansion and proper ciliogenesis (Molla-Herman et al., 2010). A ciliary-pocket-like structure that does not support vesicular trafficking forms during vertebrate spermiogenesis as a consequence of the inward movements of the basal body toward the nucleus followed by the caudal extension of the cell body (Fawcett and Bedford, 1979). However, in vertebrate spermatids, the cell membrane surrounds the axoneme and grows in concert with the elongating microtubules. Thus in this case, the ciliary pocket is a transitory structure that changes dimensions and then disappears. In *Drosophila* spermatids, only the distal end of the elongating axoneme is surrounded by an inner membrane that remains contiguous with the outer plasma membrane throughout the assembly of the axoneme (Fritz-Niggli and Suda, 1972; Tokuyasu, 1975). Cold exposure revealed that the CPL held both stable and unstable axonemal microtubules. The latter population regrew quickly after recovery from cold treatment, suggesting that tubulin addition occurs in the distal-most end of the CPL. This agrees with previous findings showing that the elongation of flagellar axoneme occurs at its distal tips, with the addition of specific components that are translocate at the microtubule plus ends (Rosenbaum and Witman, 2002).

The disorganized symmetry of the axoneme and the isolated A-tubules at the distal end of the CPL suggest that each microtubule doublet grows asynchronously. Longitudinal sections often revealed isolated A-tubules ending in a moderately dense material at the tip of the axoneme that might be implicated in microtubule nucleation. The wall of the A-tubules might act as template for the B-tubules that, in turn, could support the growth of the C-blade that gives continuity to the longitudinal sheets emerging from the C-tubules of the centriole. Similar conclusions come from structural analysis of procentriole formation in human cultured cells (Guichard et al., 2010). However, the polymerization of B- and C-tubules is bidirectional in cultured cells, whereas B-tubules and C-blades elongate at their distal or plus ends in the *Drosophila* spermatid axoneme.

Materials and Methods

Drosophila strains

The stock containing the Unc-GFP transgene and the *unc*^{2} mutant was described previously (Baker et al., 2004). *Klp10A* mutation was reported previously (Delgehyr et al., 2012). Flies were raised on standard *Drosophila* medium at 24℃.

Immunofluorescence preparations

Testes from third-instar larvae and pupae were dissected in PBS and placed in a small drop of 5% glycerol in PBS on a glass slide. Testes were squashed under a small cover glass and frozen in liquid nitrogen. After removal of the coverslip, the samples were immersed in methanol for 10 minutes at −20℃. For localization of microtubules, the samples were washed for 15 minutes in PBS and incubated for 1 hour in PBS containing 0.1% BSA (PBS-BSA) to block nonspecific staining. The samples were incubated overnight for 1 hour at room temperature with mouse anti-acetylated tubulin (1:100; Sigma-Aldrich) in a humid chamber. After washing in PBS-BSA the samples were incubated for 1 hour at room temperature with Alexa Fluor 555 secondary antibodies (1:800; Invitrogen). DNA was visualized with incubation for 3–4 minutes in Hoechst stain. Testes were mounted in small drops of 90% glycerol in PBS. Images were taken by using an Axio Imager Z1 (Carl Zeiss) microscope using 100× objective and equipped with an HBO 50 W mercury lamp for epifluorescence and with an AxioCam HR cooled charge-coupled camera (Carl Zeiss). Gray-scale digital images were collected separately and then pseudocolored and merged using Adobe Photoshop 7.0 software (Adobe Systems).

Microtubule regrowth assays

Testes from third-instar larvae and pupae expressing Unc-GFP were dissected in PBS and placed on ice for 45 minutes to depolymerize the microtubules. Testes were then placed at 24℃ for 5 minutes, fixed and immunostained for acetylated tubulin as described above.

Transmission electron microscopy

Testes isolated from larvae and pupae were fixed in 2.5% glutaraldehyde buffered in PBS overnight at 4℃. After the pre-fixation, the material was carefully rinsed in PBS and post-fixed in 1% osmium tetroxide in PBS for 2 hours at 4℃. Samples were then washed in the same buffer, dehydrated in a graded series of ethanol, embedded in a mixture of Epon-Araldite, and polymerized at 60℃ for 48 hours. Thin sections (50–60 nm thick) were obtained with a Reichert Ultracut E ultramicrotome equipped with a diamond knife, mounted upon copper grids, stained routinely with uranyl acetate and lead citrate, and then observed with a Philips CM 10 transmission electron microscope operating at an accelerating voltage of 80 kV and with a Tecnai Spirit Transmission Electron Microscope (FEI) operating at 100 kV equipped with a Morada CCD camera (Olympus).

Acknowledgements

We are grateful to Tomer Avidor-Reiss and Maurice Kernan for sharing mutant stocks.

Author contributions

M.G.R. and G.C. conceived the project. M.G. and M.G.R. performed experiments. G.C. wrote the manuscript.

Funding

This work was supported by PRIN2009 to G.C.

References

Avidor-Reiss, T., Maer, A. M., Koundakjian, E., Polyanovsky, A., Keil, T., Subramaniam, S. and Zuker, C. S. (2004). Decoding cilia function: defining specialized genes required for compartmentalized cilia biogenesis. *Cell* **117**, 527-539.

Baker, J. D., Adhikarakunnathu, S. and Kernan, M. J. (2004). Mechanosensory-defective, male-sterile unc mutants identify a novel basal body protein required for ciliogenesis in Drosophila. *Development* **131**, 3411-3422.

Benmerah, A. (2013). The ciliary pocket. *Curr. Opin. Cell Biol.* **25**, 78-84.

Bisgrove, B. W. and Yost, H. J. (2006). The roles of cilia in developmental disorders and disease. *Development* **133**, 4131-4143.

Carvalho-Santos, Z., Machado, P., Alvarez-Martins, I., Gouveia, S. M., Jana, S. C., Duarte, P., Amado, T., Branco, P., Freitas, M. C., Silva, S. T. et al. (2012). BLD10/CEP135 is a microtubule-associated protein that controls the formation of the flagellum central microtubule pair. *Dev. Cell* **23**, 412-424.

Czarnecki, P. G. and Shah, J. V. (2012). The ciliary transition zone: from morphology and molecules to medicine. *Trends Cell Biol.* **22**, 201-210.

Dawe, H. R., Farr, H. and Gull, K. (2007). Centriole/basal body morphogenesis and migration during ciliogenesis in animal cells. *J. Cell Sci.* **120**, 7-15.

Delgehyr, N., Rangone, H., Fu, J., Mao, G., Tom, B., Riparbelli, M. G., Callaini, G. and Glover, D. M. (2012). Klp10A, a microtubule-depolymerizing kinesin-13, cooperates with CP110 to control Drosophila centriole length. *Curr. Biol.* **22**, 502-509.

Enjolras, C., Thomas, J., Chhin, B., Cortier, E., Duteyrat, J. L., Soulavie, F., Kernan, M. J., Laurençon, A. and Durand, B. (2012). Drosophila chibby is required for basal body formation and ciliogenesis but not for Wg signaling. *J. Cell Biol.* **197**, 313-325.

Fabian, L. and Brill, J. A. (2012). Drosophila spermiogenesis: Big things come from little packages. *Spermatogenesis* **2**, 197-212.

Fawcett, D. and Bedford, J. (1979). *The Spermatozoon: Maturation, Motility, Surface Properties and Comparative Aspects*. Baltimore, MD: Urban & Schwarzenberg.

Fisch, C. and Dupuis-Williams, P. (2011). Ultrastructure of cilia and flagella - back to the future! *Biol. Cell* **103**, 249-270.
Fritz-Niggli, H. and Suda, T. (1972). Bildung und Bedeutung der Zentriolen: Eine Studie und Neuinterpretation der Meiose von Drosophila. [Formation and significance of centrioles: A study and new interpretation of the meiosis of Drosophila]. *Cytobiologie* **5**, 12-41.
Fuller, M. T. (1993). Spermatogenesis. In *The Development of Drosophila melanogaster* (ed. M. Martinez-Arias and M. Bate), pp. 71-147. Cold Spring Harbor, NY: Cold Spring Harbor Laboratory Press.
Gilula, N. B. and Satir, P. (1972). The ciliary necklace. A ciliary membrane specialization. *J. Cell Biol.* **53**, 494-509.
Gluenz, E., Höög, J. L., Smith, A. E., Dawe, H. R., Shaw, M. K. and Gull, K. (2010). Beyond 9+0: noncanonical axoneme structures characterize sensory cilia from protists to humans. *FASEB J.* **24**, 3117-3121.
Guichard, P., Chrétien, D., Marco, S. and Tassin, A. M. (2010). Procentriole assembly revealed by cryo-electron tomography. *EMBO J.* **29**, 1565-1572.
Han, Y. G., Kwok, B. H. and Kernan, M. J. (2003). Intraflagellar transport is required in Drosophila to differentiate sensory cilia but not sperm. *Curr. Biol.* **13**, 1679-1686.
Hennig, W. and Kremer, H. (1990). Spermatogenesis of Drosophila hydei. *Int. Rev. Cytol.* **123**, 129-175.
Ishikawa, H. and Marshall, W. F. (2011). Ciliogenesis: building the cell's antenna. *Nat. Rev. Mol. Cell Biol.* **12**, 222-234.
Kim, S. and Tsiokas, L. (2011). Cilia and cell cycle re-entry: more than a coincidence. *Cell Cycle* **10**, 2683-2690.
Kobayashi, T. and Dynlacht, B. D. (2011). Regulating the transition from centriole to basal body. *J. Cell Biol.* **193**, 435-444.
Kozminski, K. G., Johnson, K. A., Forscher, P. and Rosenbaum, J. L. (1993). A motility in the eukaryotic flagellum unrelated to flagellar beating. *Proc. Natl. Acad. Sci. USA* **90**, 5519-5523.
Molla-Herman, A., Ghossoub, R., Blisnick, T., Meunier, A., Serres, C., Silbermann, F., Emmerson, C., Romeo, K., Bourdoncle, P., Schmitt, A. et al. (2010). The ciliary pocket: an endocytic membrane domain at the base of primary and motile cilia. *J. Cell Sci.* **123**, 1785-1795.
Nigg, E. A. and Raff, J. W. (2009). Centrioles, centrosomes, and cilia in health and disease. *Cell* **139**, 663-678.
Pazour, G. J., Dickert, B. L., Vucica, Y., Seeley, E. S., Rosenbaum, J. L., Witman, G. B. and Cole, D. G. (2000). Chlamydomonas IFT88 and its mouse homologue, polycystic kidney disease gene tg737, are required for assembly of cilia and flagella. *J. Cell Biol.* **151**, 709-718.
Pedersen, L. B. and Rosenbaum, J. L. (2008). Intraflagellar transport (IFT) role in ciliary assembly, resorption and signalling. *Curr. Top. Dev. Biol.* **85**, 23-61.
Pedersen, L. B., Veland, I. R., Schrøder, J. M. and Christensen, S. T. (2008). Assembly of primary cilia. *Dev. Dyn.* **237**, 1993-2006.
Reiter, J. F., Blacque, O. E. and Leroux, M. R. (2012). The base of the cilium: roles for transition fibres and the transition zone in ciliary formation, maintenance and compartmentalization. *EMBO Rep.* **13**, 608-618.
Ringo, D. L. (1967). Flagellar motion and fine structure of the flagellar apparatus in Chlamydomonas. *J. Cell Biol.* **33**, 543-571.
Riparbelli, M. G., Callaini, G. and Megraw, T. L. (2012). Assembly and persistence of primary cilia in dividing Drosophila spermatocytes. *Dev. Cell* **23**, 425-432.
Rohatgi, R. and Snell, W. J. (2010). The ciliary membrane. *Curr. Opin. Cell Biol.* **22**, 541-546.
Roque, H., Wainman, A., Richens, J., Kozyrska, K., Franz, A. and Raff, J. W. (2012). Drosophila Cep135/Bld10 maintains proper centriole structure but is dispensable for cartwheel formation. *J. Cell Sci.* **125**, 5881-5886.
Rosenbaum, J. L. and Witman, G. B. (2002). Intraflagellar transport. *Nat. Rev. Mol. Cell Biol.* **3**, 813-825.
Sarpal, R., Todi, S. V., Sivan-Loukianova, E., Shirolikar, S., Subramanian, N., Raff, E. C., Erickson, J. W., Ray, K. and Eberl, D. F. (2003). Drosophila KAP interacts with the kinesin II motor subunit KLP64D to assemble chordotonal sensory cilia, but not sperm tails. *Curr. Biol.* **13**, 1687-1696.
Silverman, M. A. and Leroux, M. R. (2009). Intraflagellar transport and the generation of dynamic, structurally and functionally diverse cilia. *Trends Cell Biol.* **19**, 306-316.
Sorokin, S. P. (1968). Reconstructions of centriole formation and ciliogenesis in mammalian lungs. *J. Cell Sci.* **3**, 207-230.
Szymanska, K. and Johnson, C. A. (2012). The transition zone: an essential functional compartment of cilia. *Cilia* **1**, 10.
Tates, A. D. (1971). *Cytodifferentiation During Spermatogenesis in Drosophila Melanogaster: An Electron Microscope Study*. PhD thesis, Rijksuniversiteit, Leiden Germany.
Tokuyasu, K. T. (1975). Dynamics of spermiogenesis in Drosophila melanogaster. VI. Significance of "onion" nebenkern formation. *J. Ultrastruct. Res.* **53**, 93-112.
Witman, G. B. (2003). Cell motility: deaf Drosophila keep the beat. *Curr. Biol.* **13**, R796-R798.